An experimental investigation on the effects of surface gravity waves on the water evaporation rate in different air flow regimes

Amin Jodat, Mohammad Moghiman & Golshad Shirkhani

Heat and Mass Transfer
Wärme- und Stoffübertragung

ISSN 0947-7411

Heat Mass Transfer
DOI 10.1007/s00231-013-1211-2

Springer

Heat Mass Transfer
DOI 10.1007/s00231-013-1211-2

ORIGINAL

An experimental investigation on the effects of surface gravity waves on the water evaporation rate in different air flow regimes

Amin Jodat · Mohammad Moghiman · Golshad Shirkhani

Received: 25 October 2012 / Accepted: 26 July 2013

Abstract Estimating rate of evaporation from undisturbed water surfaces to moving and quiet air has been the topic a vast number of research activities. The obvious presence of various shapes of gravity waves on the water body surfaces was the motivation of this experimental investigation. In this investigation experimental measurements have been done to quantify evaporation rate from wavy water surfaces in free, mixed and forced convection regimes. The effects of a wide range of surface gravity waves from low steepness, round shaped crest with slow celerity, to steep and very slight spilling crest waves, on the water evaporation rate have been investigated. A wide range of $Gr/Re^2 (0.01 \leq Gr/Re^2 \leq 100)$ was achieved by applying different air flow velocities on a large heated wave flume equipped with a wind tunnel. Results reveal that wave motion on the water surface increase the rate of evaporation for all air flow regimes. For free convection, due to the effect of wave motion for pumping rotational airflows at the wave troughs and the dominant effect of natural convection for the air flow advection, the maximum evaporation increment percentage from wavy water surface is about 70 %. For mixed and forced convection, water evaporation rate increment is more sensitive to the air flow velocity for the appearance of very slight spilling on the steep wave crests and the leeward air flow structures.

A. Jodat · M. Moghiman · G. Shirkhani (✉)
Department of Mechanical Engineering, Ferdowsi University of Mashhad, Mashhad, Iran
e-mail: Golshad.Shirkhani@gmail.com

A. Jodat
e-mail: Amin.jodat@yahoo.com

M. Moghiman
e-mail: moghiman@um.ac.ir

List of symbols

d	Still water depth (m)
g	Gravitational acceleration (m/s^2)
Gr	Mass transfer Grashof number
H	Wave height (m)
k	Wave number $(1/m)$
L	Wave length (m)
L_c	Characteristic length along the test chamber (m)
$\dot{m}_e$	Evaporation rate of water $(kg/m^2\ h)$
Nu	Nusselt number
P	Pressure (Pa)
$P_{v,s}$	Saturated vapor pressure at the water surface
$P_{v,\infty}$	Saturated vapor pressure at the ambient air
Re	Reynolds number
S	Stroke of the paddle
T	Wave period (s)
V	Velocity of air (kg/m^3)

Greek symbols

ρ	Density (kg/m^3)
μ	Dynamic viscosity (Ns/m^2)
$\bar{\rho}$	Mean mixture density of air (kg/m^3)
σ	Paddle frequency

Subscripts

g	Moist air property including dry air and water vapor
s	Properties at the surface of the water
∞	Average properties at the ambient air

1 Introduction

Evaporation from still and wavy free water surfaces is a phenomenon widely perceived in many natural and engineering aspects. Although the existence of waves on the

Published online: 21 August 2013

surface of water bodies (pools, tanks, rivers, lakes and estuaries) is obvious but corresponding to the literatures, the major efforts on the topic of water evaporation have been to acquire a correlation for estimating the rate of evaporation from still water surfaces and undisturbed water surfaces into different air flow regimes [2, 9, 11, 14–16]. Pauken [11] had an investigation for predicting the rate of evaporation from a still water heated pool into a low speed wind tunnel and the air flow regimes on the water were from free to turbulent forced convection. Shah [14–16] evaluated the correlations for the rate of evaporation from undisturbed water pools to quiet air. He verified different empirical correlations and developed various formulas for calculating the rate of evaporation to quiet air. Asdrubali [2] in an experimental investigation by varying various parameters such as water temperature, air temperature, relative humidity and air velocity, proposed a scale model to evaluate water evaporation from indoor swimming pools. Jodat et al. [9] carried out a series of experimental investigations over a wide range of water temperatures and air velocities for $0.01 \leq Gr/Re^2 \leq 100$ to represent a correlation for estimating the evaporation rate from still and rippled water surfaces. Obviously still water surface is an ideal hypothesis, rarely observed in the real industrial and natural world and it is rarely possible to find an open body of water without any disturbances or waves on the surface. Actually the interfacial surface of air and water is deformed by several shapes of waves, ranging from capillary waves of a few micrometers long to gravity waves of higher wavelengths, depending on the water depth. Dynamics of capillary waves, referred to as ripples or wavelets, are dominated by the effect of surface tension. Gravity waves induced by a mechanical force such as the prescribed motion of a wavemaker's paddle at one side of a wave flume, can be simulated in laboratories for various purposes. Herein for intermediate water depth flumes the threshold, $\frac{\pi}{10} < kd < \pi$, is considered and for deep water depth the threshold, $\pi < kd$ is considered, where $k = \frac{2\pi}{L}$ is the wave number, L is the wavelength and d is the still water depth [4].

A few investigations on the topic of mass transfer enhancement by interfacial waves have been reported [3, 7, 19]. Hopfinger and Das [7], had an experimental study on the effect of capillary waves on the rate of heat and mass transfer in a closed container and he suggested that large amplitude capillary waves increase the rate of interfacial heat and mass transfer from a volatile liquid. Das and Hopfinger [3] experimentally investigated the mass transfer enhancement by large amplitude gravity waves at a liquid–gas vapor interface. The waves were sub-harmonically excited in a circular cylinder partially filled with liquid, by oscillating the cylinder in the direction normal to the liquid surface. [19], had an experiment on the mass transfer enhancement due to surface waves at a horizontal gas–liquid interface. His results revealed that at the peak frequency of induced interfacial surface waves, independently of liquid flow rate, mass transfer increased quadratically and its maxima was approximately 45 % greater than in the absence of waves. The effects of gravity waves exposed to different air flow regimes on the water evaporation rate has not been reported corresponding to the literatures. Therefore in this experiment laboratory setups are made using a wave flume equipped with a wind tunnel to quantify the evaporation rate from wavy water surfaces exposed to different air flow regimes. The waves investigated in this experiment ranged from round shaped crest waves with long wavelengths and periods to steep and very slight spilling crest at the initial stage of breaking waves. Waves with crest angles less than 120° (angle between two lines tangent to the surface profile at the wave crest) are substantially prepared to spill [17]. Herein the effect of air velocity over steep waves at the inception of spilling process is significant [18]. In high air velocities, spilling of the wave crest can be occurred at lower steepness. The widespread investigations on the topic of wind wave interactions can be used for describing the results of the presented experiments.

The present study of evaporation measurements has been motivated by the need to investigate the effects of wave parameters and convective air flow on the water evaporation rate from wavy water surfaces. Measurements of evaporation rates are performed for wave heights ranged from $H = 0$ to 0.17 m corresponding to wave periods ranged from $T = 0.6$ to 1.8 s. The air velocities in the flume ranged from 0.05 to 5 m/s, the air temperature in the wind tunnel and the water temperature of the wave flume considered to be 25 and 25 °C respectively to achieve $0.01 \leq Gr/Re^2 \leq 100$. The experimental results of the present study are concerned with intermediate water depth $(\frac{\pi}{10} < kd < \pi)$ gravity waves.

2 Mathematical description

In the next two sections the mathematical relations between wave parameters, and the relations for describing convective air flow over the water surface are discussed respectively.

2.1 The role of wave height and period for describing surface gravity waves

The resultant wave height and wave period of progressive gravity waves on deep and intermediate water depth in a

horizontal bottom bed wave flume for a fixed paddle stroke are expressed by Eq. 1 and 2 respectively [4].

$$H = 4S\left(\frac{\sinh\ kd}{kd}\right)\frac{kh\sinh\ kd - \cos\ hkd + 1}{\sinh\ 2kd + 2kd} \tag{1}$$

$$T = \frac{2\pi}{\sqrt{gk\ \tan\ kd}} \tag{2}$$

where S is the stroke of the wavemaker's paddle and g is the gravitational acceleration. In this investigation by varying the wavemaker's paddle frequency, various wave period from $T = 0.6$ to 1.8 s is achieved. The variations of waveheight is due to the variation of wave period, the resultant wave heights are measured by two wave gauges mounted on the interfacial wavy surface of air and water (from $H = 0$ to 0.17 m). Measuring wave heights and period, the effects of $H/T\left[\frac{m}{s}\right]$ on the water evaporation rate have been investigated. For waves with high celerity and high steepness the H/T is large. On the other hand low steepness and low celerity waves have low H/T. Waves with crest angles less than 120° (angle between two lines tangent to the surface profile at the wave crest) are substantially prepared to spill [17]. Herein the effect of air velocity over steep waves at the inception of spilling process is significant [18]. In high air velocities very light spilling of the wave crest can be occurred at lower steepness. Regarding this threshold and considering intermediate depth gravity waves $\left(\frac{\pi}{10} < kd < \pi\right)$, various shapes of waves $[0 < H/T < 0.18\ \text{m/s}]$ are generated in this experiment and exposed to different air flow velocities.

2.2 Convective air flow over water surface

In order to prescribe the dominant air flow regime over the water surface, the following expression may be used;

$$\frac{Gr}{Re^2} = \frac{\text{Natural Convection Strength}}{\text{Forced Convection Strength}} \tag{3}$$

Gr and Re are the Grashof and Reynolds numbers, respectively, which are expressed as:

$$Gr = \frac{\bar{\rho}_g\left(\rho_{g,s} - \rho_{g,\infty}\right)gL_C^3}{\mu^2} \tag{4}$$

$$Re = \frac{\bar{\rho}_g V L_c}{\mu} \tag{5}$$

where $\rho_{g,s}$ and $\rho_{g,\infty}$ are the densities of moist air at the surface of water and at the ambient, respectively. V, is the air velocity, μ is the air dynamic viscosity and L_c is the characteristic length along the test chamber. The density of the moist air at the free surface is estimated as the sum of the partial densities of vapor $(\rho_{v,s})$ and dry air $(\rho_{a,s})$ as [8] :

$$\rho_{g,s} = \rho_{v,s} + \rho_{a,s} \tag{6}$$

In addition, the mean mixture of air in the boundary layer $(\bar{\rho}_g)$ is defined as [8]:

$$\bar{\rho}_g = \frac{\rho_{g,s} + \rho_{g,\infty}}{2} \tag{7}$$

In order to calculate the density of moist air, the perfect gas equation is used. In this experiment the air velocities V = 0.05 and 0.1 m/s conduct to free convection regime $(\text{Gr}/\text{Re}^2 \geq 15)$, the air velocities V = 0.9 and 2 m/s conduct to mixed convection regime, $(0.2 \leq \text{Gr}/\text{Re}^2 \leq 12)$ and the air velocities V = 4 and 5 m/s conduct to forced convection regime, $(\text{Gr}/\text{Re}^2 \leq 0.05)$.

3 Experimental setup and measurements

The experiments were performed in a wave flume equipped with a wind tunnel. A schematic of the test chamber is shown in Fig. 1. The main flume to allow prescribed deep water gravity wave generation is 10.0 m long, 0.5 m wide and 0.6 m height with two passive wave absorption zones at both ends. The still water depth is 0.35 m. The wind tunnel to allow airflow on the water waves is 2 m long 0.5 m wide and 0.8 m high. The effects of the two physical aspects on the water evaporation rate were to be examined:

- Surface gravity waves achievable by a flap type wave maker hinged at one side of the wave flume.
- Air flow regime achievable by a centrifugal blowing fan located at one side of the wind tunnel.

Waves were generated by a flap-type wave maker hinged at the bottom of the channel at one side of the flume. Rubber seals are used to minimize the water leakage from the small clearance between the edges of the wave maker's plate and the side walls of the channel. Paddle motion is generated using a four link mechanism with a controllable arm length coupled to an electric motor. By varying the rotational speed of the electric motor, various paddle motion periods (0.6–1.8 s) can be achieved. Wave heights were measured by two capacitance wave gauges located at the interfacial surface of air and water. Regarding the mathematical description of gravity waves, various wave heights with respect to the wave period can be achieved (0–0.17 m). A faster paddle motion may result in larger values of $H/T(0 < H/T < 0.18\ \text{m/s})$.

A blowing centrifugal fan was used to control the air velocity within the chamber. The air flows through air heaters and then through grid shelves to decrease turbulent effects within the chamber. The air flows on a 2 m long of the chamber and then exits. The air velocity within the

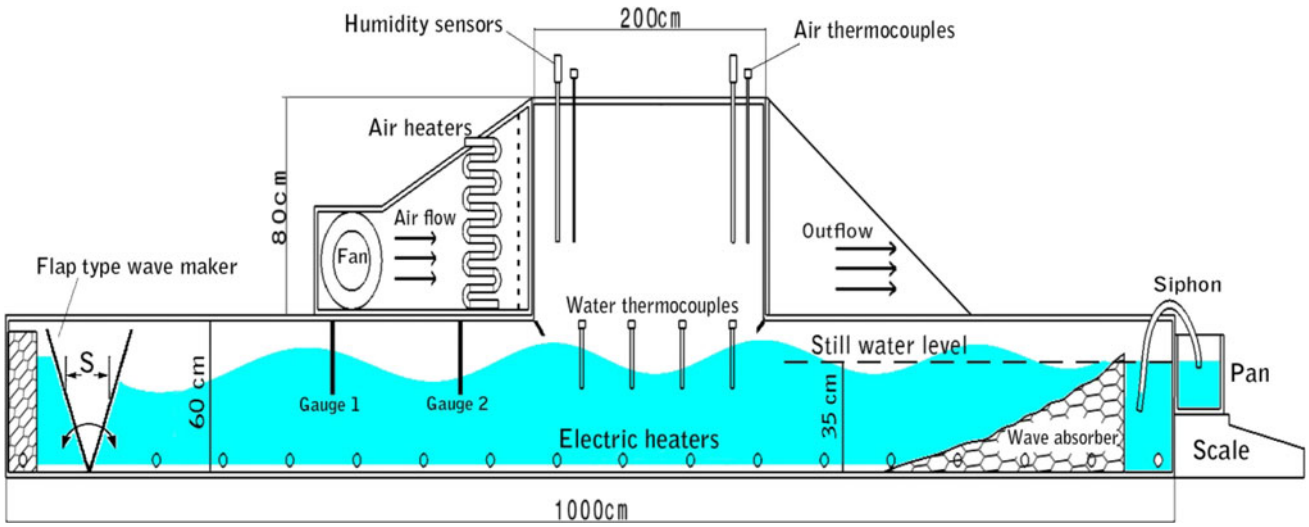

Fig. 1 A schematic of the experimental setup. The drawing is not to scale

chamber was measured using a thermal anemometer, at nine locations across the wind tunnel above the water surface, and the maximum deviation observed was less than 10 %. The average air velocities considered were $0.05, 0.1, 0.9, 2, 4,$ and 5 m/s. The inlet air relative humidity was controlled using a conventional air conditioning system. A barometer was used to measure the total pressure of the laboratory for each experiment. Air relative humidity was measured by two sensors placed near the inlet and outlet of the wind tunnel, above the water surface. In addition, the air temperature measured by thermocouples located over the wind tunnel, considered to be 25 °C.

Immersion heaters were installed near the bottom of the flume to elevate the bulk temperature of the flume to the desired conditions. They were low heat flux heaters with 2,500 W of total power. The heaters were made of nichrome wire encased in poly (tetra fluoroetylene) spaghetti tubing. The mean water temperature was measured by averaging the readings of T-type thermocouples that were placed on the water surface. The flume was divided into eight equal square sections and one thermocouple was placed in the center of each section. The water temperature considered to be 35 °C. A thermoregulation system was used to guarantee a temperature oscillation of water of about ±0.1 °C from the fixed value.

The evaporation rate was evaluated based on two methods; First, by means of the flow rate measurement and the difference between the inlet and outlet absolute humidity. Second, by means of a small pan connected to the main flume via a siphon tube [12]. The evaporation rate was calculated based on weighing this small pan using a digital scale over a 10 min period of time. The maximum capacity and the resolution of the scale were about 4 kg and 0.01 g, respectively. However, when the evaporation rate was too slow the measurements were recorded on an hourly basis. The description of the measuring devices and their accuracy and the ranges of measurements is presented in Table 1. All the measuring instruments were calibrated before the experiments were performed and the data generated by these instruments was captured using a PC data acquisition system.

4 Results and discussion

A wide range of surface gravity waves from round shaped crest, low steepness and slow celerity waves for low values of H/T, to steep and very slight spilling crest at the initial stage of breaking waves, for high values of H/T, are generated and exposed to different air flow regimes namely free, mixed and forced convection $(0.01 \leq Gr/Re^2 \leq 100)$, to reveal the effects of the wave parameters and air flow regimes on the rate of water evaporation. Measurements of evaporation rates are performed for wave heights ranged

Table 1 The description of the measuring devices with their accuracies and the ranges of measurements

The measuring devices	Range	Accuracy
Temperature sensors	−45 to 135 °C	±0.2 °C
Humidity sensors	1–99 %	±1 % RH
Thermal anemometer	1–10 m/s	±0.04 m/s
Digital balance	0–6 kg	± 0.1 g
Immersion heaters	0–2,500 W	PID
Air heaters	0–2,000 W	PID
Wave gage	200 samples/s	±1 mm
Inverter	0–3,000 rpm	1 rpm

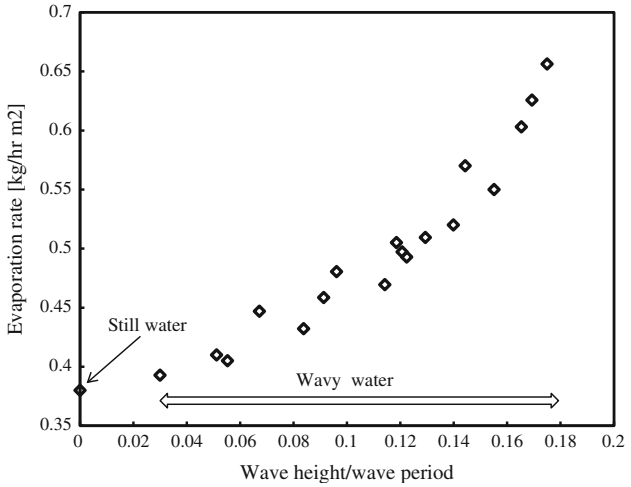

Fig. 2 Comparison of the measured evaporation rates between still water (no wave) and wavy water surface for free convection regime ($V = 0.05$ m/s)

from $H = 0$ to 0.17 m corresponding to wave periods ranged from $T = 0.6$ to 1.8 s.

4.1 Free convection regime

Figure 2 shows the comparison of the measured evaporation rates between still water (no wave present on the surface) and wavy water surfaces, for different H/T values ($0 < H/T < 0.18$ m/s). The air velocity over gravity waves is $V = 0.05$ m/s and correspondingly, $Gr/Re^2 = 100$. It can be seen that the evaporation rate from wavy water is higher than that from still water surface. This fact can be occurred due to two reasons, (1) deformation and enhancement of interfacial area between air and water. (2) Enhancement of convective heat transfer due to rotational flows and coherent structures of airflow induced by surface waves [10]. Figure 3 shows the increment percentages of evaporation rate and interfacial surface area due to presence of gravity waves on the water surface for the free convection regime. This figure reveals that the average value of the interfacial area increment percentage is approximately 2 % while the average value of evaporation increment percentage is about 30 %. This emphasizes that the effect of rotational air flows induced by wavy water surface on the evaporation increment is much more than the effect of interfacial area increment. This figure also indicates that an increase in H/T values of the gravity waves (causing steeper and faster waves), increases evaporation rate up to 80 percent compared with the still water evaporation rate.

The effects of H/T and air velocity on the water evaporation rate for free convection regime (air velocities: V = 0.05 and 0.1 m/s) is plotted in Fig. 4. It is observed that the evaporation rate increases as the air velocity and the H/T values increase. The trend line's concavity is upward for all values of H/T and the slope of the trend line increases by increasing H/T. This is due to the behavior of wave motion for pumping vortices near the interfacial surface [18] and the dominant effect of natural convection for the air mass advection [5]; for free convection regime, the rotational flows at the wave troughs accompanied by an increase in pressure drop. This pressure drop can increase the evaporation rate. Moreover, for very high values of the H/T parameter, where the waves are faster and steeper, due to very light spilling of the wave crests and droplet splash into the air stream, faster evaporation can be occured [1]. For the free convection regime, at $H/T =$ 0.172 m/s, very light spilling at the wave crests appears in this experiment. Herein the effect of the wave crests

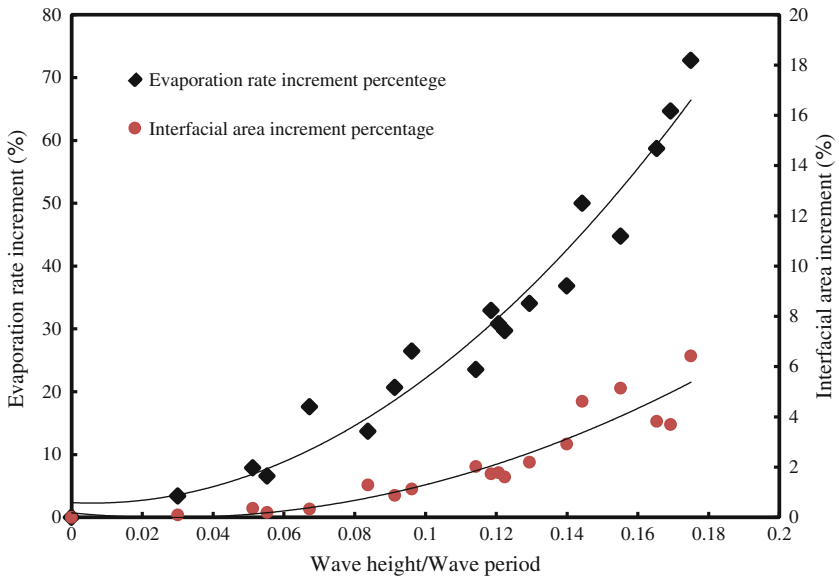

Fig. 3 The increment percentages of evaporation rate and interfacial contact area due to waves for free convection regime ($V = 0.05$ m/s)

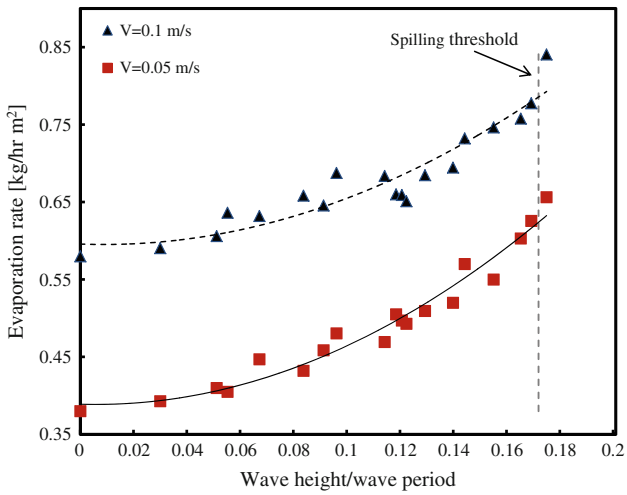

Fig. 4 Effect of H/T and air velocity on water evaporation rate for free convection regime

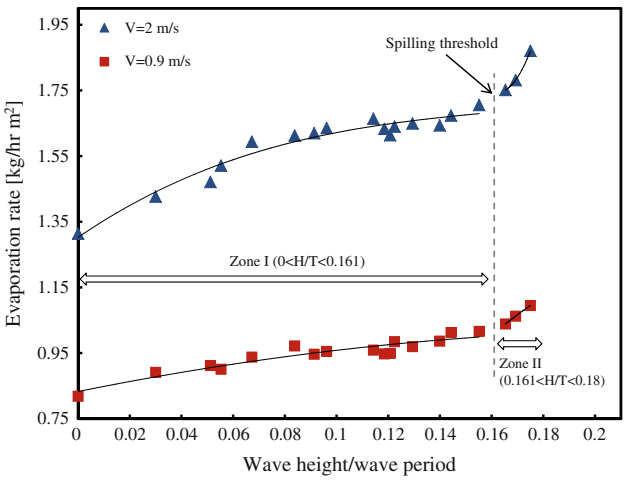

Fig. 5 Variation of water evaporation rate with two ranges of H/T values, before and after the slight crest spilling of waves in mixed convection regime

spilling is much more for high air velocities (specially for the forced convection regime).

4.2 Mixed convection regime

Figure 5 demonstrates the effects of H/T and air velocity on water evaporation rate for mixed convection regime (air velocities: V = 0.9 and 2 m/s). In comparison with Fig. 4, it is obvious that for mixed convection regime the trend line's curve consists of two concavities: downward (before the appearance of slight spilling on the wave crests) and upward (after the crest spilling). Based on the first appearance of the waves crest spilling, the increasing process of H/T is divided into two zones: zone I and zone II. The increasing process of evaporation rate at zone I, has a lower slope compared with that of zone II. It is suggested that, as the waves exposing to the air flow, become steeper and faster, regions of quite air forms at the leeward of waves and the local trapped air forms an effective barrier to the vertical transport of water vapor [6]. In comparison with the free convection regime, the slightly spilling on the wave crests occurs at a lower value of H/T (for mixed convection at $H/T = 0.161$ m/s wave crest spills slightly). This fact is due to the effect of the air flow over steep wave crests. The slope of the increasing process of evaporation rate rises up at zone II. This can be occurred because for high H/T values, steep wave crest and the instantaneous airflow cause crests spilling and droplet splash slightly into the air stream. Air flow separation occurs behind steep wave crests and the separation bubble is strongly unsteady Reul et al. [13]. These flow structures which are intermittent in time and space on the wave current, greatly increase the rate of evaporation (Fig. 6).

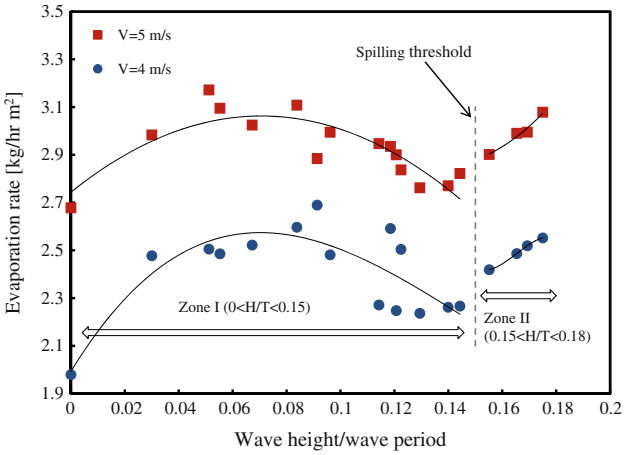

Fig. 6 Variations of water evaporation rate in forced convection regime, by two ranges of H/T values, before and after slight crest spilling of waves

4.3 Forced convection regime

Figure 7 shows the effects of H/T and air velocity on water evaporation rate for forced convection regime (air velocities: V = 4 and 5 m/s). In comparison with Fig. 5 it is obvious that the water evaporation rate variation in Fig. 7 is more sensitive to H/T, the trend line's concavities are more intense and the wave crest spilling occurs at a lower value of $H/T (H/T = 0.15$ m/s), this value is lower than the ones for free and mixed convection because of the higher air velocities over wave crests. Considering the wave spilling thresholds, the increasing process of H/T is divided into two zones: zone I (downward concavity) and zone II (upward concavity). The decreasing slope of the trend line at zone I is due to the wave leeward vortices, as mentioned for the mixed convection. The leeward air

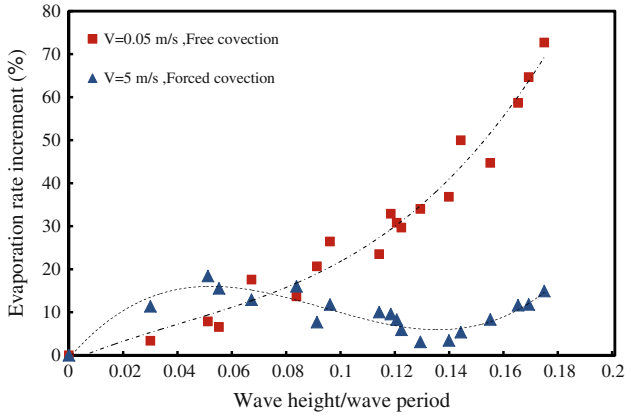

Fig. 7 The increment percentages of evaporation rate due to waves for free and forced convection regimes

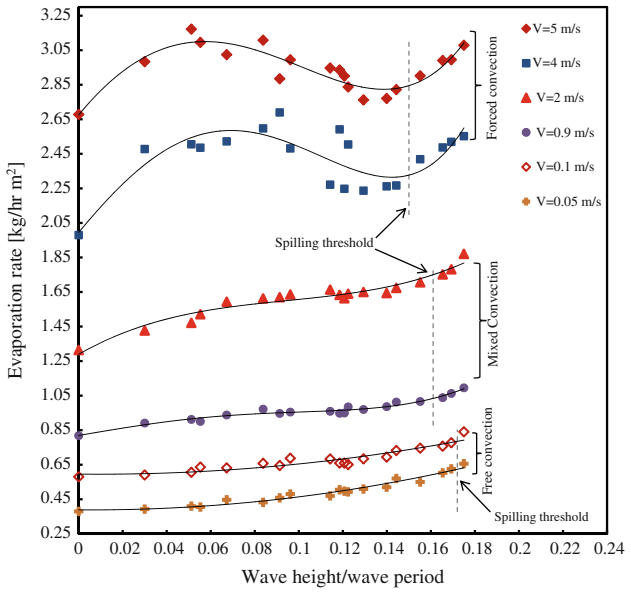

Fig. 8 Effect of the wave parameter H/T, and air velocity on water evaporation rate

structures are larger and more stable for the higher values of air velocities [13] and these stable vortices strongly resist upward vertical motion of vapor droplets. The vapour droplets trapped at the leeward of waves due to the swirl motion of the airstream. Reul et al. [13] has captured air velocity and vorticity distributions above gravity waves in a wind-wave tank via digital particle image velocimetry technique (DPIV) and presence of these swirl motion of airstream at the leeward of waves was evident in his experiment. At zone II, after the wave crest spilling, wave motions pump droplet spray into the turbulent air flow and the evaporation rate increases again. The variation of the water evaporation rate for the forced convection is strongly dependent on the airflow structures over the waves. Although the amounts of evaporation rate due to different wave shapes are higher for high air velocities, but the evaporation increment percentage compared with still water for high air velocities is lower than that for low air velocities. Figure 7 shows the increment percentages of evaporation rate due to waves for free and forced convection regimes. For low values of H/T, slow celerity and low steepness waves, the evaporation increment percentage for forced convection is higher than that for free convection, but for steeper and faster waves, due to the air swirl motion and local trapped vapour droplet at the wave troughs, the evaporation increment percentage for forced convection, is lower than that for free convection.

5 Conclusions

The effects of a wide range of surface gravity waves from low steepness, round shaped crest with slow celerity waves for low values of the *waveheight*/*waveperiod*, H/T, to steep and very slight spilling crest at the initial stage of breaking waves, for high values of H/T, on the water evaporation rate in free, mixed and forced convection regimes have been investigated experimentally. It is concluded that wavy water surfaces increase the evaporation rate and the air flow regimes over the waves can greatly affect the rate of evaporation for different variety of wave parameters. Figure 8 shows levels of evaporation rate for different air flow regimes. Based on the presented results, the following conclusions may be drawn:

- In all flow regimes, the water evaporation rate increases by increasing H/T values.
- For free convection regime ($15 < Gr/Re^2$) the effect of wave motion for pumping vortices of air flow at the wavy interfacial surfaces on the water evaporation increment is more than the effect of interfacial aera increment percentage.
- For mixed convection regime due to higher air velocities, the evaporation rate increases when compared with that of free convection regime.
- For forced convection regime, at low values of $H/T (H/T < 0.06)$ the very high air velocity has the dominant effect on water evaporation rate increment, at medium values of $H/T (0.06 < H/T < 0.14)$ the leeward air flow structures which form barrier for the vertical transport of vapor decrease water evaporation rate and finally at high values of $H/T (0.14 < H/T)$, appearance of spilling on the wave crests causes high increases in evaporation rate
- For all flow regimes, at higher air velocities, spilling of the wave crest can be occurred at lower values of H/T.

Acknowledgments The authors wish to express their sincere thanks to Ferdowsi University of Mashhad, who has financially supported the project (Grant No. 1/16560).

References

1. Andreas EL, Edson JB, Monahan EC, Rouault MP, Smith SD (1995) The spray contribution to net evaporation from the sea: a review of recent progress. Bound Layer Meteorol 72:3–52
2. Asdrubali F (2009) A scale model to evaluate water evaporation from indoor swimming pools. Energy Build 41:311–319
3. Das S, Hopfinger E (2009) Mass transfer enhancement by gravity waves at a liquid-vapour interface. Int J Heat Mass Transf 52:1400–1411
4. Dean RG, Dalrymple RA (1991) Water wave mechanics for engineers and scientists, vol 2. World Scientific Publishing Company Incorporated
5. Dellil AZ, Azzi A, Jubran BA (2004) Turbulent flow and convective heat transfer in a wavy wall channel. Heat Mass Transf 40:793–799
6. Ding F, Wan W, Yuan H (2003) The influence of background winds and attenuation on the propagation of atmosferic gravity waves. J Atmos Solar-Terr Phy 65:857–869
7. Hopfinger E, Das S (2009) Mass transfer enhancement by capillary waves at a liquid–vapour interface. Exp Fluids 46:597–605
8. Iskra CR, Simonson CJ (2007) Convective mass transfer coefficient for a hydrodynamically developed airflow in a short rectangular duct. Int J Heat Mass Transf 50:2376–2393
9. Jodat A, Moghiman M, Anbarsooz M (2012) Experimental comparison of the ability of Dalton based and similarity theory correlations to predict water evaporation rate in different convection regimes. Heat Mass Transf 48:1397–1406
10. Kruse N, Rudolf von Rohr P (2006) Structure of turbulent heat flux in a flow over heated wavy. Int J Heat Mass Transf 49:3514–3529
11. Pauken MT (1998) An experimental investigation of combined turbulent free and forced evaporation. Exp Thermal Fluid Sci 18:334–340
12. Boukadida N, Nasrallah SB (2001) Mass and heat transfer during water evaporation in laminar flow inside a rectangular channel-validity of heat and mass transfer analogy. Int J Thermal Sci 40:67–81
13. Reul N, Branger H, Giovanangeli JP (2008) Air flow structure over short-gravity breaking water waves. Bound Layer Meteorol 126:477–505
14. Shah M (2002) Rate of evaporation from undisturbed water pools to quiet air: evaluation of available correlations. Int J HVAC&R Res 8:125–131
15. Shah MM (2008) Analytical formulas for calculating water evaporation from pools. Heat Piping Air Cond Eng 114:610–618
16. Shah MM (2012) Improved method for calculating evaporation from indoor water pools. Energy Build 49:306–309
17. Stewart RH (2004) Introduction to physical oceanography. A&M University, Texas
18. Sullivan PP, McWilliams JC (2010) Dynamics of winds and currents coupled to surface waves. Annu Rev Fluid Mech 42:19–42
19. Vázquez-Uṇa G, Chenlo-Romero F, Sanchez-Barral M, Pérez-Muṇuzuri V (2000) Mass transfer enhancement due to surface wave formation at a horizontal gas-liquid interface. Chem Eng Sci 55:5851–5856